Available online at www.sciencedirect.com
SCIENCE DIRECT
Solid State Communications 134 (2005) 89–95
solid state communications
www.elsevier.com/locate/ssc

Variable resistance at the boundary between semimetal and excitonic insulator

Massimo Rontani[a,*], L.J. Sham[b]

[a]INFM National Center on nanoStructures and bioSystems at Surfaces (S3), Via Campi 213/A, 41100 Modena, Italy
[b]Department of Physics, University of California San Diego, La Jolla, CA 92093-0319, USA

Received 6 July 2004; accepted 12 July 2004 by the guest editors
Available online 5 January 2005

Abstract

We solve the two-band model for the transport across a junction between a semimetal and an excitonic insulator. We analyze the current in terms of two competing terms associated with neutral excitons and charged carriers, respectively. We find a high value for the interface resistance, extremely sensitive to the junction transparency. We explore favorable systems for experimental confirmation.

PACS: 72.10.Fk; 73.40.Cg; 73.40.Ns; 73.50.Lw

Keywords: A. Semiconductors; A. Surfaces and interfaces; D. Electron–electron interactions; D. Electronic transport

1. Introduction

The concept that excitons can condense in a semimetal (SM) and form an *excitonic insulator* (EI), if the energy band overlap is small compared to their binding energy, dates back to the sixties [1]. Experimental evidence has been put forward for the exciton phase [2], but the EI state remains a mystery. Moreover, the possibility of experimental discrimination between the EI and the ordinary dielectric has been called into question [3]. We demonstrate that, if an EI exists, it develops unusual transport properties that make it qualitatively different from an ordinary insulator.

Elsewhere [23], we considered, in a two-band model, a junction between a SM and a semiconductor, whose small gap originates from the renormalization of the SM energy bands due to: (i) hybridization of conduction and valence bands, (ii) electron–hole pairing driving the EI condensation. Carriers incident on the interface from the SM side with energies below the gap are backscattered again into the SM, possibly into a different band. We found that interband scattering only occurs for (ii), due to the proximity of the EI which broadens the interface potential profile.

Here we focus on the latter case only. We analyze the current generated by a bias voltage across a clean SM/EI junction as two competing terms associated with neutral excitons and charged carriers, respectively. Below the EI gap, carriers are backscattered by the interface with energy band branch crossing. The formalism is similar to that for the metal/superconductor (NS) interface [4], and indeed we find the same dependence of transmission and reflection coefficients on the quasi-particle energy ω. However, while electrons below the superconducting gap are Andreev-reflected as holes, carriers reflected below the EI gap conserve their charge and the electric current is zero. Above the gap, when charge transmission is allowed, an unusually high electrical resistance remains. We find that the electrons that are backscattered from one band to another are equivalent to incoming holes correlated with the incoming electrons. When such pairs enter the condensate they are converted into an exciton supercurrent, in such a way that

* Corresponding author.
E-mail address: rontani@unimore.it (M. Rontani).

0038-1098/$ - see front matter © 2004 Elsevier Ltd. All rights reserved.
doi:10.1016/j.ssc.2004.07.076

the electron–hole flow across the sample is conserved. The latter exciton channel is preferred with respect to charge transmission, even if ω is just slightly above the gap. Therefore, the additional resistance arises due to the competition of exciton and charge currents, reminiscent of the interplay between electric supercurrent and heat flow at the NS junction. The effect is smeared as an insulating overlayer is inserted at the interface, spoiling the transparency of the junction: in the tunneling limit, exciton transport is suppressed. We further discuss physical systems which could show the effects our theory predicts.

The paper is organized as follows: In Section 2 we describe the solution of the electron transmission through the interface in terms of the two-band model of the SM/EI junction and in Section 3 we analyze the transport in terms of charge and exciton currents and examine the role of the exciton coherence. Then we study the interface differential conductance (Section 4), and lastly we review candidate experimental systems (Section 5).

2. Transport across the interface

We consider a junction made of a semimetal and an excitonic insulator. Specifically, the EI band structure originates from the renormalization of the SM energy bands, driven by Coulomb interaction. The EI gap corresponds to the binding energy of the electron–hole pairs which form a condensate. The interface discontinuity is solely brought about by the variation of the electron–hole pairing potential, $\Delta(z)$. This kind of junction could be experimentally realized by applying a pressure gradient or by inhomogeneously doping a sample grown by means of epitaxial techniques (see Section 5).

The electron and hole Fermi surfaces of the SM on the junction left-hand side are taken to be perfectly nested, the effective masses of the two bands being isotropic and equal to m. The quasi-particle excitations across the interface must satisfy the mean-field equations

$$\omega f(z) = -\frac{1}{2m}\left[\frac{\partial^2}{\partial z^2} + k_{\mathrm{F}}^2\right] f(z) + \Delta(z) g(z), \tag{1a}$$

$$\omega g(z) = \frac{1}{2m}\left[\frac{\partial^2}{\partial z^2} + k_{\mathrm{F}}^2\right] g(z) + \Delta(z) f(z), \tag{1b}$$

with k_{F} Fermi wave vector and $\hbar = 1$. The amplitudes f and g are the position-space representation of the electron quasi-particle across the interface: $|f|^2$ ($|g|^2$) is the probability for an electron of being in the conduction (valence) band, with energy $\omega > 0$ referenced from the chemical potential, which is in the middle of the EI gap due to symmetry. We assume Δ is a step function, $\Delta(z) = \Delta\theta(z)$.

In the elastic scattering process at the interface, all relevant quasi-particle states are those degenerate—with energy ω—on both sides of the junction. We handle the interface by matching wave functions of the incident, transmitted, and reflected particles at the boundary. In the bulk EI, there are a pair of magnitudes of k associated with ω, namely

$$k^+ = \sqrt{2m}\sqrt{k_{\mathrm{F}}^2/2m \pm (\omega^2 - \Delta^2)^{1/2}}. \tag{2}$$

The total degeneracy of relevant states for each ω is fourfold: $\pm k^{\pm}$. The two states $\pm k^+$ have a dominant conduction-band character, while the two states $\pm k^-$ are mainly valence-band states. Using the notation

$$\Psi(z) = \begin{pmatrix} f(z) \\ g(z) \end{pmatrix} \tag{3}$$

the wave functions degenerate in ω are

$$\Psi_{\pm k^+} = \begin{pmatrix} u_0 \\ v_0 \end{pmatrix} \mathrm{e}^{\pm \mathrm{i} k^+ z}, \quad \Psi_{\pm k^-} = \begin{pmatrix} v_0 \\ u_0 \end{pmatrix} \mathrm{e}^{\pm \mathrm{i} k^- z}, \tag{4}$$

with the amplitudes u_0, v_0 defined as

$$u_0 = \sqrt{\frac{1}{2}\left[1 + \frac{(\omega^2 - \Delta^2)^{1/2}}{\omega}\right]},$$
$$v_0 = \sqrt{\frac{1}{2}\left[1 - \frac{(\omega^2 - \Delta^2)^{1/2}}{\omega}\right]}, \tag{5}$$

possibly extended in the complex manifold. With regards to the SM bulk, $\Delta = 0$ and the two possible magnitudes of the momentum q reduce to $q^{\pm} = [2m(k_{\mathrm{F}}^2/2m \pm \omega)]^{1/2}$, with wave functions

$$\Psi_{\pm q^+} = \begin{pmatrix} 1 \\ 0 \end{pmatrix} \mathrm{e}^{\pm \mathrm{i} q^+ z}, \quad \Psi_{\pm q^-} = \begin{pmatrix} 0 \\ 1 \end{pmatrix} \mathrm{e}^{\pm \mathrm{i} q^- z}, \tag{6}$$

for conduction and valence bands, respectively.

The effect of an insulating layer or of localized disorder at the interface is modeled by a δ-function potential, namely $V(z) = H\delta(z)$ The appropriate boundary conditions, for particles traveling from SM to EI are as follows: (i) continuity of Ψ at $z = 0$, so $\Psi_{\mathrm{EI}}(0) = \Psi_{\mathrm{SM}}(0) \equiv \Psi(0)$. (ii) $[f'_{\mathrm{EI}}(0) - f'_{\mathrm{SM}}(0)]/(2m) = Hf(0)$ and $[g'_{\mathrm{EI}}(0) - g'_{\mathrm{SM}}(0)]/(2m) = -Hg(0)$, the derivative boundary conditions appropriate for δ-functions [5]. (iii) Incoming (incident), reflected and transmitted wave directions are defined by their group velocities. We assume the incoming conduction band electron produces only outgoing particles, namely an electron incident from the left can only produce transmitted particles with positive group velocities $v_{\mathrm{g}} > 0$ and reflected ones with $v_{\mathrm{g}} < 0$.

Consider an electron incident on the interface from the SM with energy $\omega > \Delta$ and wave vector q^+. There are four channels for outgoing particles, with probabilities A, B, C, D, and wave vectors q^-, $-q^+$, k^+, $-k^-$, respectively. In other words, C is the probability of transmission through the interface with a wave vector on the same (i.e., forward) side of its Fermi surface as q^+ (i.e., $q^+ \to k^+$, not $-k^-$), while

D gives the probability of transmission on the back side of the Fermi surface (i.e., $q^+ \to -k^-$). B is the probability of intraband reflection, while A is the probability of reflection on the forward side of the Fermi surface (interband scattering from conduction to valence band). We write the steady state solution as

$$\Psi_{\mathrm{SM}}(z) = \Psi_{\mathrm{inc}}(z) + \Psi_{\mathrm{refl}}(z), \quad \Psi_{\mathrm{EI}}(z) = \Psi_{\mathrm{trans}}(z),$$

where

$$\Psi_{\mathrm{inc}}(z) = \begin{pmatrix} 1 \\ 0 \end{pmatrix} e^{iq^+ z},$$

$$\Psi_{\mathrm{refl}}(z) = a \begin{pmatrix} 0 \\ 1 \end{pmatrix} e^{iq^- z} + b \begin{pmatrix} 1 \\ 0 \end{pmatrix} e^{-iq^+ z}, \tag{7}$$

$$\Psi_{\mathrm{trans}}(z) = c \begin{pmatrix} u_0 \\ v_0 \end{pmatrix} e^{ik^+ z} + d \begin{pmatrix} v_0 \\ u_0 \end{pmatrix} e^{-ik^- z}.$$

Applying the boundary conditions, we obtain a system of four linear equations in the four unknowns a, b, c, and d, which we solve at a fixed value for ω. We introduce the dimensionless barrier strength $Z = mH/k_F = H/v_F$, where v_F is the Fermi velocity. The quantities A, B, C, D, are the ratios of the probability current densities of the specific transmission or reflection channels to the current of the incident particle, e.g. $A = |J_A/J_{\mathrm{inc}}|$, and so on. The conservation of probability requires that

$$A + B + C + D = 1. \tag{8}$$

This result is useful in simplifying expressions for energies below the gap, $\omega < \Delta$, where there can be no transmitted electrons, so that $C = D = 0$. Then, Eq. (8) reduces simply to $A = 1 - B$.

The Andreev approximation [4] consists in letting $k^+ = k^- = q^+ = q^- = k_F$ in Eq. (7), on the basis that the ratio $\Delta/|G|$ is small, where G is the band overlap of the SM. Fig. 1 compares results obtained in the framework of the Andreev approximation (thin lines) with data computed without any constraint on momenta of quasi-particles (thick lines), at $\Delta/|G| = 0.1$. While the agreement at $Z = 0$ is satisfactory, the coefficients at $Z = -1$ deviate significantly for energies above the gap. Note that, whatever the value of $\Delta/|G|$ or Z is, the full numerical calculation always gives finite values for B and D, contrary to the approximate analytic results according to which $B = D = 0$ when $Z = 0$. As the ratio $\Delta/|G|$ increases, the agreement between approximate and full solutions turns out to be increasingly worse.

If the junction is clean ($Z = 0$, left panel of Fig. 1), below the gap, $\omega < \Delta$, only interband reflection is possible. Even above the gap, $\omega > \Delta$, there is a high probability for interband reflection, which strongly depends on ω: for energies close to the gap, $\omega \approx \Delta$ reflection is almost certain, $A \approx 1$. Remarkably, transmission probability $C \approx 1 - A$ increases very slowly with ω, which is the cause for the high value of resistance. The effect is washed out by the opacity of the interface: as $|Z|$ increases ($Z = -1$, right panel of Fig. 1), transmission probability loses its dependence on ω, and reflection channel turns from interband, A, into intraband type, B.

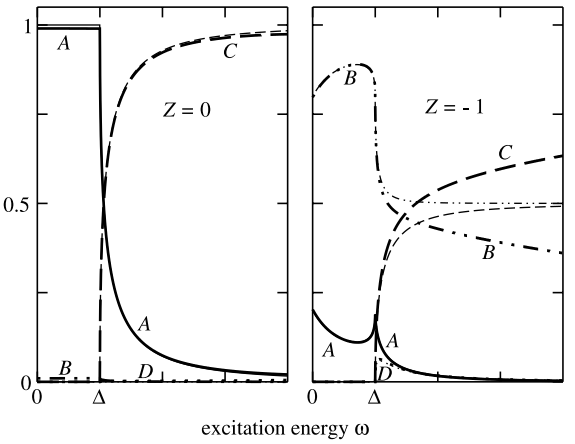

Fig. 1. Plot of transmission and reflection coefficients at SM/EI boundary computed both in the Andreev approximation (thin lines) and taking exactly into account the wave vectors of scattered particles (thick lines). Only in the latter case the coefficients depend on $\Delta/|G|$ (we take $\Delta/|G| = 0.1$). Left: $Z = 0$. Right: $Z = -1$. A gives the probability of interband reflection, B gives the probability of ordinary intraband reflection, C gives the transmission probability without branch crossing, and D gives the probability of transmission with branch crossing. The parameter Z measures the interface transparency.

Results obtained for the SM/EI junction by means of the Andreev approximation are formally identical to those of the NS interface, as given in Table II of Ref. [6]. However, there are a few differences in the dependence of the NS coefficients on Z with respect to the present case, which is due to different boundary conditions, as stressed in note [5]. While the NS coefficients are even functions of Z, in the SM/EI case A and B do not have a definite parity with respect to the sign of Z for $\omega < \Delta$, while for $\omega > \Delta$, A, B, C, and D are even in Z. Nevertheless, the expressions for coefficients in the strong barrier case coincide with the corresponding ones for the NS case. Therefore, apart from some differences for small values of Z, the physical role of the barrier is the same in both cases.

3. Charge versus exciton current

We describe the interband reflection process in terms of a neutral electron–hole current. The probability density $\rho_{\mathrm{e-h}}(z,t)$ for finding either a conduction-band electron or a valence-band hole at a particular time and place is $\rho_{\mathrm{e-h}}(z,t) = |f|^2 + 1 - |g|^2$. We consider conduction electrons with crystal momentum with modulus larger than k_F, otherwise we define $\rho_{\mathrm{e-h}}(z,t)$ as $\rho_{\mathrm{e-h}}(z,t) = 1 - |f|^2 + |g|^2$. We obtain, in the first case,

$$\frac{\partial \rho_{e-h}}{\partial t} + \frac{\partial J_{e-h}}{\partial z} = 0, \quad J_{e-h} = J_{pair} + J_{cond}, \tag{9}$$

where $J_{pair} = m^{-1}\mathrm{Im}\{f^* \partial f/\partial z + g^* \partial g/\partial z\}$ is the density current of the electron–hole pair, and the term $\partial J_{cond}/\partial z = -4\,\mathrm{Im}\{f^* g \Delta\}$ explicitly depends on the built-in coherence of the electron–hole condensate Δ. While J_{pair} is analogous to the standard particle current $J = m^{-1}\,\mathrm{Im}\{f^*\,\partial f/\partial z - g^*\,\partial g/\partial z\}$ except a difference in sign, the term J_{cond} is qualitatively different and is attributed to the exciton supercurrent of the EI ground state.

If $\omega < \Delta$ and $Z = 0$, each wave function (7), solution of Eqs. (1a) and (1b), carries zero total electric current eJ, which is the sum of the equal and opposite incident and reflected fluxes, and finite and constant electron–hole current $J_{e-h} = 2v_F$. Inside the SM side ($z < 0$), the supercurrent contribution J_{cond} is zero. Note that J_{e-h} conserves its constant value, independent of z, since quasi-particle states (7) are stationary. In fact, as the contribution to the electron–hole current J_{pair} vanishes approaching the boundary, J_{pair} is rapidly converted into the supercurrent J_{cond}. Excitons therefore can flow into the EI side without any resistance, and the sum J_{e-h} of the two contributions, J_{pair} and J_{cond}, is constant through all the space.

As an example, consider the quasi-particle steady state of Eq. (7) and the coefficients a, b, c, d obtained in the 'Andreev approximation' (Section 2). For $\omega < \Delta$, k^+ and k^- in the excitonic insulator have small imaginary part which lead to an exponential decay on a length scale λ, where

$$\lambda = \frac{v_F}{2\Delta}\left(1 - \frac{\omega^2}{\Delta^2}\right)^{-1/2}. \tag{10}$$

The quasi-particles penetrate a depth λ before the electron–hole current J_{pair} is converted to a supercurrent J_{cond} carried by the condensate; right at the gap edge the length diverges. For clarity, we define C and D here as the transmission probabilities at $z \gg \lambda$ while for $\omega > \Delta$ plane-wave currents are spatially uniform and we need not specify the position at which they are evaluated.

When there is no barrier at the interface, $Z = 0$, the steady state (7) is specified by $b = d = 0$, $a = v_0/u_0$, and $c = 1/u_0$. Below the gap coherence factors u_0 and v_0 are complex and equal in modulus. For $\omega < \Delta$, $|a|^2 = 1$ which means the incident conduction-band electron is totally reflected into the SM valence band. Thus, the electron–hole current J_{pair} carried in the semimetal equals $2v_F$, but J_{pair} of the excitonic insulator is exponentially small for $z \gg 0$. Explicitly,

$$J_{pair} = \frac{|c|^2}{m}(|u_0|^2 + |v_0|^2)\mathrm{Im}\left[(e^{ik^+ z})^* \frac{\partial}{\partial z}(e^{ik^+ z})\right].$$

Letting $k^+ \approx k_F + i/(2\lambda)$, we have

$$J_{pair} = 2v_F\, e^{-z/\lambda}. \tag{11}$$

The 'disappearing' electron–hole current reappears as exciton current carried by the condensate. Recalling the definition of J_{cond},

$$\partial J_{cond}/\partial z = -4\,\mathrm{Im}\{f^* g \Delta\},$$

by integration we obtain

$$J_{cond} = -4\Delta|c|^2 \int_0^z dz'\, e^{-z'/\lambda}\,\mathrm{Im}[u_0^* v_0]$$
$$= 2v_F(1 - e^{-z/\lambda}). \tag{12}$$

This is the desired result, explicitly showing the supercurrent J_{cond} increasing to an asymptotic value as $z \to \infty$, at the same rate as the quasi-particle current J_{pair} dies away.

Above the gap, $\omega > \Delta$, J increases from zero and J_{e-h} decreases. However, close to the gap, electron transmission to the EI side is still inhibited ($C \approx 0$) by the pairing between electrons and holes of the condensate: an electron can stand alone and carry current only after its parent exciton has been 'ionized' by injecting -say- a conduction-band electron or by filling a valence-band hole in the EI. The ionization costs an amount of energy of the order of the binding energy of the exciton, Δ. Therefore, as long as $\omega \approx \Delta$, the competition between exciton and electron flow favors interband reflection, which is the source of the high electric resistance.

4. Differential conductance at finite voltage

Electric transport across the SM/EI interface is the experimental signature of the physics we have previously discussed. When a bias voltage V is applied across the junction, non-equilibrium quasi-particle populations are generated, which can be found in principle only by implementing a self-consistent scheme linking the computation of both charge and potential. Here we adopt a simplified approach assuming ballistic acceleration of particles except for the scattering at the interface. This should be a good approximation for the case, e.g., of a thin junction connecting massive electrodes, as long as the diameter of the orifice is small compared to a mean-free path. In addition, we assume that the distribution functions of all incoming particles are given by equilibrium Fermi functions, apart from the energy shift due to the accelerating potential. We choose the electrochemical potential in the EI as our reference level, being a well defined quantity at finite temperature T, when carriers are provided by thermal excitations.

The computation of the electric current I follows step by step the analogous treatment in the superconductor case [6,7]. Here we only state the result for the differential conductance, $\partial I/\partial V$, which in ordinary units is

$$\frac{\partial I}{\partial V} = e^2 W N(\varepsilon_F)\frac{v_F}{4}\int_{-\infty}^{\infty} d\omega \xi(\omega)[C(\omega)$$
$$+ D(\omega)]\left[-\frac{\partial f(\omega')}{\partial \omega'}\right]_{\omega' = \omega - eV}, \tag{13}$$

where $C(\omega)$ and $D(\omega)$ are taken to be even functions defined over the whole real axis, $f(\omega)$ is the Fermi distribution function, $\xi(\omega)$ is the channel degeneracy which takes the value one (two) if $|\omega|>|G|/2$ ($|\omega|<|G|/2$), W is the interface cross-sectional area, and $N(\varepsilon_F)$ is the density of states per volume at the Fermi energy per each semimetal band. Eq. (13) is derived assuming that the transmission coefficients are independent of V. At $T=0$ the function $-\partial f/\partial\omega$ appearing in Eq. (13) turns into a Dirac's delta, while at finite T one must perform the integration over ω and the overall effect is that sharp energy features of $\partial I/\partial V$ are smeared out. We focus exclusively on the zero temperature case.

Fig. 2 shows the differential conductance $\partial I/\partial V$ of the SM/EI interface at $T=0$ as a function of the bias voltage and for different values of Z. The calculation has been carried out in the Andreev approximation. The current shows an activated behavior, the threshold being the energy gap Δ. When the interface is clean ($Z=0$), the conductance slowly rises with the voltage V, due to the additional resistance brought about by the interband reflection mechanism. In fact, $\partial I/\partial V$ goes like $(|eV|-\Delta)^{1/2}$, as discussed in Section 2. As the interface opacity gradually increases (going from $Z=0.3$ up to $Z=3$) we note the following two features: (i) curves become progressively more and more flat, with a well defined step at the threshold Δ. Therefore, the additional resistance close to the gap, which is responsible for the gradual increase of $\partial I/\partial V$, is completely suppressed in the tunneling regime. The opacity of the interface spoils the spatial coherence between the SM and EI sides and inhibits the transport channel A. (ii) All curves tend asymptotically, for large voltages, to a limiting value which is the contact resistance of the interface when there is no electron–hole condensate present ($\Delta=0$), namely $\partial I/\partial V = e^2WN(\varepsilon_F)v_F/2(1+Z^2)$. Indeed, at high energies the effect of the electron–hole condensate is negligible—while it is dominant close to Δ—as Z increases, the contact resistance decreases as Z^{-2} (see the expressions for C and D coefficients for large values of Z in Table II of Ref. [6]).

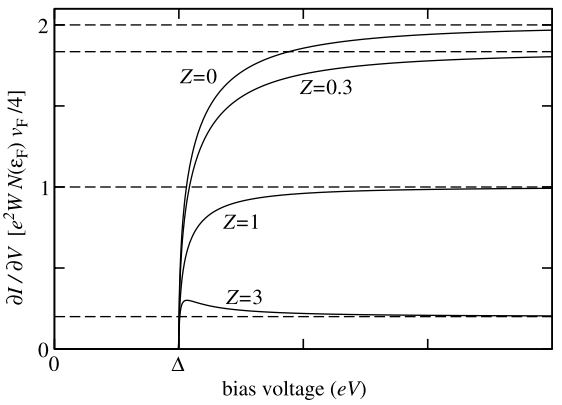

Fig. 2. Plot of differential conductance, $\partial I/\partial V$, computed at zero temperature in the Andreev approximation, as a function of the bias voltage applied at SM/EI boundary for several values of the barrier transparency Z. Curves for different values of Z at large voltages tend to asymptotic values (dashed lines) given by the contact resistance of the junction in the absence of the electron–hole condensate ($\Delta=0$). The differential conductance is given in units of $e^2WN(\varepsilon_F)v_F/4$, where W is the interface cross-sectional area, v_F is the Fermi velocity, and $N(\varepsilon_F)$ is the density of states per volume at the Fermi energy per each semimetal band.

5. Choice of physical systems

We address the question of which systems should be considered for the experimental realization of the SM/EI junction. The physical quantity which we suggest to measure is the junction electrical resistance, in particular the differential conductance as a function of the applied voltage. We showed this quantity, at $T=0$ and for different amounts of interface disorder, in Fig. 2. By measuring the current we *indirectly* probe the effect of the neutral exciton supercurrent, which is responsible for the loss of conductance at voltages close to the gap. In such an experiment it would be important to track the evolution of conductance as disorder is added to the interface.

5.1. Rare-earth calcogenides

Presently, the strongest experimental evidence of the existence of the EI phase concerns rare-earth calcogenides such as $TmSe_xTe_{1-x}$ [2], $Sm_{1-x}La_xS$ [2,8], $Sm_{1-x}Tm_xS$, YbO and YbS [8]. These intermediate valent compounds all crystallize in the NaCl structure and undergo a semimetal/semiconductor transition under pressure, since the band overlap G can be changed from negative to positive values by applying high hydrostatic pressure to the sample, while the dielectric screening does not change dramatically, since the gap is indirect [2]. According to resistivity and Hall mobility measurements [2], at low temperatures one intercepts the EI phase close to $G\approx 0$. Here we focus on the most studied $TmSe_{0.45}Te_{0.55}$ alloy, but the discussion could apply to other compounds as well.

When the gap of $TmSe_{0.45}Te_{0.55}$ is closing with external pressure, an indirect band gap develops between the highest valence Tm $4f^{13}$ level Γ_{15} at the Γ point and the minimum of the Δ_2 conduction band 5d states at the X point of the Brillouin zone [2]. Since the otherwise localized 4f band is broadened and shows a maximum at Γ due to p(Se,Te)−f(Tm) covalent hybridization [10], we suggest to realize a SM/EI interface by varying the hydrostatic pressure applied to a $TmSe_{0.45}Te_{0.55}$ sample along the [100] direction. Temperature and pressure values at which the junction could operate are easily deduced from the phase diagram shown in Fig. 1 of Ref. [9]. For example, a pressure of 14 kbar guarantees that the compound remains semimetallic from 5 to 300 K, while a slight decrease in pressure enters the EI phase at low temperatures.

5.2. Vertical transport in layered graphite

A single planar sheet of graphite is a zero-overlap semimetal. Conduction and valence band energy surfaces, in the proximity of the Fermi energy, form specular cones whose apexes touch in the two inequivalent points K and K', located at the corners of the hexagonal two-dimensional Brillouin zone. These essential-degeneracy points map into each other by a rotation of $2\pi/6$ [11]. Interestingly, Coulomb interaction is long ranged due to the lack of conventional screening [12]. Khveshchenko [12] claims that graphite hides a latent excitonic insulator instability. According to Ref. [12], the ground state could be a charge density wave alternating between the two inequivalent triangular sublattices, its characteristic wave vector in reciprocal space connecting K and K'. A stack of graphite layers in a staggered (ABAB…) configuration, with the atoms located in the centers and corners of the hexagons in two adjacent layers, respectively, could stabilize the EI phase by enforcing interlayer Coulomb interaction. Also doping could strengthen the EI ground state inducing exciton ferromagnetism [13]. This theory seems to explain magnetic correlations recently measured in highly oriented pyrolitic graphite [14].

We observe that in common layered samples with AB stacking graphite is a finite-overlap semimetal with very low carrier concentration, due to the small interlayer tunneling [15]. The high-symmetry P line connecting K and H points on the border vertical edge of the three-dimensional Brillouin zone has still two-fold degeneracy in energy for symmetry reasons [16], but, due to small band dispersion driven by interlayer coupling, there is a closed Fermi surface around K and a hole pocket centered at H. By moving along P one crosses both electron and hole pockets: the two-dimensional case is recovered when the interlayer distance increases indefinitely, namely H coincides with K. Therefore, we propose to fabricate a SM/EI graphite-based junction by arranging a stacking sequence where doping or interlayer interaction can be artificially controlled. Transport occurs in the stacking vertical direction: the bottom of the relevant conduction band on the SM side of the junction is located at K point, while the top of valence band at H' where H' lies on the P$'$ line including the inequivalent point K'.

5.3. Lateral junction of coupled quantum wells

Bilayers where electrons and holes are spatially separated constitute very interesting systems to test ideas presented in this work, since exciton condensation appears to have been observed in these systems [17]. In coupled quantum well heterostructures a quasi two-dimensional semimetal can be realized such that the negative gap G is indirect in *real* space, the valence band edge in one layer being higher in energy than the conduction band bottom in the other layer (Fig. 3(a)). Below we explain how our theory

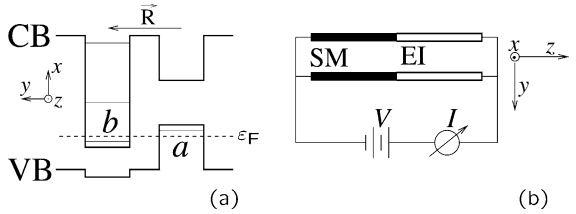

Fig. 3. (a) Energy band scheme along the growth direction of a typical semimetal bilayer heterostructure. a and b label the highest-energy valence sub-band in one layer and the lowest-energy conduction sub-band in the other layer, respectively. The motion is confined in the y (growth) direction, and it is two dimensional in the xz plane. The SM/EI interface lies in the xy plane, and $\mathbf{R}$ is the distance vector between the two layers in real space. (b) Experimental setup to measure the interface electrical resistance. A small bias voltage V is laterally applied to both layers forming the semimetal/excitonic insulator interface, and an electric current I flows across the interface.

can be extended to bilayers in a straightforward way. Several experimental setups have been proposed in order to achieve exciton condensation in such systems, including $In_{1-x}Ga_xAs/AlSb/GaSb_{1-y}As_y$ Type-IIB and biased modulation-doped GaAs/AlGaAs coupled quantum wells, and doping (n–i–p–i) superlattices [18–22]. There are several advantages in this scheme. One is that it is possible to enhance the exciton binding energy by both quantum confinement and minimization of interlayer tunneling [18,19]. The latter is most conveniently realized by interposing a wide-gap layer acting as a barrier between the two quantum wells: the thinner the layer, the stronger the Coulomb electron–hole attraction. Tunneling must be inhibited to reduce interband virtual transitions that increase the screening of Coulomb interaction, which can be accomplished by increasing the height of the inter-well potential barrier [18]. Another key point is that the semiconductor-to-semimetal transition can be driven either by manipulating the layer thickness and material composition or by continuously tuning an external electric field applied along the growth direction [20]. Last but not least, high mobility and low carrier density in state-of-the-art heterostructures are certainly favorable toward exciton condensation [22].

We propose to fabricate a lateral SM/EI junction starting from coupled quantum wells (Fig. 3). Conduction and valence band electrons laterally move in the xz plane in spatially separated quantum wells, while the interface plane xy extends parallel to the growth direction (see Fig. 3). Contrary to the model of Section 2, where conduction- (b) or valence-band (a) electrons can overlap in direct space, different bands imply now spatial separation. Therefore, the origin of the position vector $\mathbf{r}$ for the b-electron in one layer now is shifted by the amount $\mathbf{R}$ with respect to position of the a-electron in the other layer (see Fig. 3(a)). Besides, the role of an interband hybridization potential $V_{\mathrm{hyb}}(\mathbf{k})$ is now played by the hopping matrix element connecting the two

layers via tunneling. Taking further into account that the motion is quasi two dimensional (see Ref. [20] for the appearance of structure factors in the effective Coulomb interaction term), equations of motion (1) for quasiparticles still hold. The junction could be realized starting from a coupled quantum well where exciton condensation has been supposedly achieved and then destroying pairing in one region of the sample. A method could be, for example, to apply a local external electric field along the growth direction to increase band overlap [20] and therefore dielectric screening in order to suppress Δ. Electrodes should allow to apply a small bias voltage along the lateral direction (Fig. 3(b)). In addition to the interface resistance measurement, this setting nicely allows for comparison between the effects of electron–hole pairing and those of band hybridization, which have been the object of a recent controversy in cyclotron resonance experiments [21,22]. In particular, the resistance measurement we propose is able to elucidate the nature of the gap that forms in a nominally semimetallic material.

Acknowledgements

This work is supported by MIUR Progetto Giovani Ricercatori and MIUR FIRB-RBAU01ZEML. M.R. thanks E. Randon, E.K. Chang, B.I. Halperin, and C. Tejedor for stimulating discussions.

References

[1] For a review: see B.I. Halperin, T.M. Rice, Solid State Phys. 21 (1968) 115; S.A. Moskalenko, D. Snoke, Bose Einstein Condensation of Excitons and Biexcitons, Cambridge University Press, Cambridge, 2001. Section 10.3.
[2] B. Bucher, P. Steiner, P. Wachter, Phys. Rev. Lett. 67 (1991) 2717; P. Wachter, A. Jung, P. Steiner, Phys. Rev. B 51 (1995) 5542.
[3] R.R. Guseinov, L.V. Keldysh, Zh. Eksp. Teor. Fiz. 63 (1972) 2255 English transl.: Soviet Phys.-JETP 36 (1973) 1193.
[4] A.F. Andreev, Zh. Eksperim. Teor. Fiz. 46 (1964) 1823 English transl.: Soviet Phys.-JETP 19 (1964) 1228.
[5] The latter boundary condition differs in sign from the one appropriate to the metal/superconductor junction, as outlined in Ref. [6].
[6] G.E. Blonder, M. Tinkham, T.M. Klapwijk, Phys. Rev. B 25 (1982) 4515.
[7] Massimo Rontani, L.J. Sham, Appl. Phys. Lett. 77 (2000) 3033; Massimo Rontani, L.J. Sham, cond-mat/0309687.
[8] P. Wachter, J. Alloys Compd 225 (1995) 133.
[9] P. Wachter, B. Bucher, J. Malar, Europhys. Lett. 62 (2003) 343.
[10] H.J.F. Jansen, A.J. Freeman, R. Monnier, Phys. Rev. B 31 (1985) 4092.
[11] F. Bassani, G. Pastori Parravicini, Electronic States and Optical Transitions in Solids, Pergamon Press, Oxford, 1975.
[12] D.V. Khveshchenko, Phys. Rev. Lett. 87 (2001) 246802.
[13] B.A. Volkov, Yu.V. Kopaev, A.I. Rusinov, Zh. Eksp. Teor. Fiz. 68 (1975) 1899 English transl.: Soviet Phys.-JETP 41 (1976) 952; E. Bascones, A.A. Burkov, A.H. MacDonald, Phys. Rev. Lett. 89 (2002) 86401.
[14] Y. Kopelevich, P. Esquinazi, J.H.S. Torres, S. Moehlecke, J. Low Temp. Phys. 119 (2000) 691.
[15] M.S. Dresselhaus, G. Dresselhaus, Adv. Phys. 30 (1981) 139.
[16] W. Jones, N.H. March, Theoretical Solid State Physics, vol. 2, Dover, New York, 1973. App. G12.
[17] L.V. Butov, C.W. Lai, A.L. Ivanov, A.C. Gossard, D.S. Chemla, Nature 417 (2002) 47.
[18] S. Datta, M.R. Melloch, R.L. Gunshor, Phys. Rev. B 32 (1985) 2607.
[19] X. Zhu, J.J. Quinn, G. Gumbs, Solid State Commun. 75 (1990) 595; X. Xia, X.M. Chen, J.J. Quinn, Phys. Rev. B 46 (1992) 7212.
[20] Y. Naveh, B. Laikhtman, Appl. Phys. Lett. 66 (1995) 1980; Y. Naveh, B. Laikhtman, Phys. Rev. Lett. 77 (1996) 900.
[21] J.-P. Cheng, J. Kono, B.D. McCombe, I. Lo, W.C. Mitchel, C.E. Stutz, Phys. Rev. Lett. 74 (1995) 450.
[22] L.J. Cooper, N.K. Patel, V. Drouot, E.H. Linfield, D.A. Ritchie, M. Pepper, Phys. Rev. B 57 (1998) 11915; T.P. Marlow, L.J. Cooper, N.K. Patel, D.M. Whittaker, E.H. Linfield, D.A. Ritchie, M. Pepper, Phys. Rev. Lett. 82 (1999) 2362.
[23] M. Rontani, L.J. Sham, unpublished.